

Theory of coherent control with quantum light

This content has been downloaded from IOPscience. Please scroll down to see the full text.

2017 New J. Phys. 19 013009

(<http://iopscience.iop.org/1367-2630/19/1/013009>)

View [the table of contents for this issue](#), or go to the [journal homepage](#) for more

Download details:

IP Address: 163.1.203.50

This content was downloaded on 23/02/2017 at 09:19

Please note that [terms and conditions apply](#).

You may also be interested in:

[Nonlinear and quantum optics with whispering gallery resonators](#)

Dmitry V Strekalov, Christoph Marquardt, Andrey B Matsko et al.

[Integrated photonic quantum random walks](#)

Markus Gräfe, René Heilmann, Maxime Lebugle et al.

[Photon transport in a one-dimensional nanophotonic waveguide QED system](#)

Zeyang Liao, Xiaodong Zeng, Hyunchul Nha et al.

[Output field-quadrature measurements and squeezing in ultrastrong cavity-QED](#)

Roberto Stassi, Salvatore Savasta, Luigi Garziano et al.

[Photon statistics of intense entangled photon pulses](#)

Frank Schlawin and Shaul Mukamel

[Multimode theory of single-photon subtraction](#)

V Averchenko, C Jacquard, V Thiel et al.

[Spatio-temporal coherent control of atomic systems](#)

H Suchowski, A Natan, B D Bruner et al.

[Engineered quantum dot single-photon sources](#)

Sonia Buckley, Kelley Rivoire and Jelena Vukovi

[Physical background for parameters of the quantum Rabi model](#)

I D Feranchuk, A V Leonov and O D Skoromnik



PAPER

Theory of coherent control with quantum light

Frank Schlawin^{1,2} and Andreas Buchleitner¹¹ Physikalisches Institut, Albert-Ludwigs-Universität Freiburg, Hermann-Herder-Straße 3, D-79104 Freiburg, Germany² Clarendon Laboratory, University of Oxford, Parks Road, Oxford OX1 3PU, United KingdomE-mail: frank.schlawin@physics.ox.ac.uk**Keywords:** coherent control, entangled photons, quantum enhancement

RECEIVED

20 March 2016

REVISED

20 December 2016

ACCEPTED FOR PUBLICATION

28 December 2016

PUBLISHED

12 January 2017

Original content from this work may be used under the terms of the [Creative Commons Attribution 3.0 licence](#).

Any further distribution of this work must maintain attribution to the author(s) and the title of the work, journal citation and DOI.



Abstract

We develop a coherent control theory for multimode quantum light. It allows us to examine a fundamental problem in quantum optics: what is the optimal pulse form to drive a two-photon-transition? In formulating the question as a coherent control problem, we show that—and quantify how much—the strong frequency quantum correlations of entangled photons enhance the transition compared to shaped classical pulses. In ensembles of collectively driven two-level systems, such enhancement requires nonvanishing interactions.

1. Introduction

The nonlinear interaction between faint light and matter on a single atom/molecule and few-photon level is of great fundamental and practical interest: while Gedanken experiments involving single photons and single quantum emitters have recently come within reach of experimental verification [1–3], similar applications in single molecule spectroscopy may unravel the quantum dynamics of photo-sensitive materials beyond the ensemble average [4], and promise to elucidate, for instance, the role of fluctuations in energy transport [5, 6]. Similarly, few-photon experiments in nonlinear media are able to create an effective interaction between photon pairs, and are employed to construct all-optical transistors [7–12]. Clearly, the feeble probe and signal fields in such experiments pose a formidable challenge: in order to detect the typically very weak nonlinear effects at small photon numbers (on the order of one), one seeks to, either, optimize the nonlinearity of the optical medium, or to manipulate the light fields: the former route includes the cavity-enhanced coupling of light to the medium [13–15], or the enhancement of the medium's nonlinearity by additional strong driving fields [7, 8], large dipoles in highly excited Rydberg states [16, 17], or molecular design of target molecules [18, 19]. In the latter route, strong focussing of the light beams, i.e. the choice of a suitable geometry, was exploited to detect the nonlinear response on a single molecule level [1–3].

Here we present an alternative approach to enhance nonlinear interactions specifically in the highly relevant regime of weak intensities, by employing ideas from coherent control [20–22]. Whereas coherent control originally employs strong classical pulses to manipulate the interference between different excitation pathways, recent advances in the manipulation of the two-photon wavefunction of time–frequency entangled photons [23–26] open the possibility to apply coherent control techniques to interactions on the single-photon level. We will demonstrate that quantum-mechanical entanglement between photons can enhance the efficiency of the photons in carrying out a given task beyond the classically achievable limit (i.e. induced by optimally shaped pulses). Incidentally, our results challenge commonly held beliefs in coherent control, according to which the quantum nature of light is detrimental [22], and open a new avenue for exploiting quantum correlations in the control of molecular processes.

Specifically, we examine a prototypical example of nonlinear light–matter interaction—the resonant two-photon absorption in a three-level system driven by either photon pairs [27] or famished ‘classical’ coherent light pulses [28]. The three-level system represents the simplest theoretical model to feature a two-photon transition, and will allow us to extract the impact of quantum correlations in the most transparent way. Using a

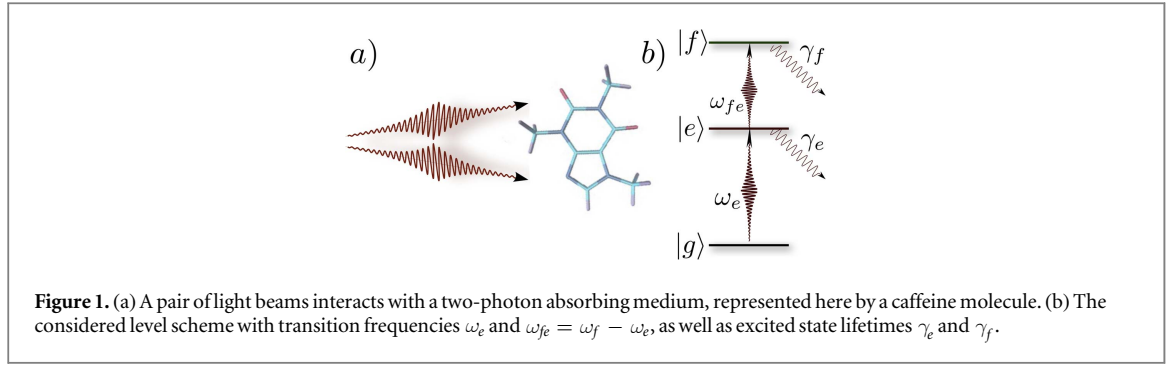


Figure 1. (a) A pair of light beams interacts with a two-photon absorbing medium, represented here by a caffeine molecule. (b) The considered level scheme with transition frequencies ω_e and $\omega_{fe} = \omega_f - \omega_e$, as well as excited state lifetimes γ_e and γ_f .

variational approach, we derive optimal pulse forms for classical and quantum two-photon states, in order to excite the target state f at a given time t . Our analytical results demonstrate that the optimal pulse form is, in general, given by an entangled two-photon state. Only if the matter system consists of an ensemble of noninteracting two-level atoms, classical light can perform as well as quantum light.

Note, in contrast, that it is well known that the two-photon absorption rate scales linearly with the pump intensity creating the entangled photons, while it scales quadratically for classical pulses [29]. Yet this scaling behavior, which originates in the creation process, cannot per se be attributed to entanglement per se. Indeed, with the right choice of parameters, downconversion can produce separable two-photon states [30], which nevertheless scale linearly in the pump intensity. Let us also mention that similar, yet different, scenarios as compared to the present one have been considered earlier in the literature: Dayan [31] theoretically analyzed off-resonant two-photon absorption (i.e. with the intermediate state far off-resonant) of multimode quantum light, and concluded that ‘excluding the linear intensity dependence of the coherent signal, all the other effects considered in this paper are completely described within the classical framework’, and ‘can be created by appropriately shaping classical pulses’. Our results show that this claim does not hold in the resonant case. Finally, let us stress that our present study concerns the quantum correlations between photons (as controlled by shaping their spectral features), rather than quantum fluctuations within predefined modes, which also have been studied elsewhere, and which also report an enhancement due to squeezed light with the same mean photon number as a coherent reference state [32–34].

2. Two-photon absorption

We consider a system of three electronic states with a ground state g , intermediate states e , and target state f as depicted in figure 1(b). The system is illuminated by two (possibly quantum) light fields, described by field operators $\hat{E}_{1,2}(\omega)$. It is initialized in the ground state, and our goal consists in maximizing the population in state f at time t by controlling the joint quantum state ψ of the two light fields. To this end, we consider the functional

$$J[\psi] = \langle \hat{p}_f(t) \rangle_\psi - \lambda (\langle \hat{n}_1 \hat{n}_2 \rangle_\psi - N^2). \quad (1)$$

The first term in equation (1), $\langle \hat{p}_f(t) \rangle_\psi$, denotes the probability of the system to be in the target state f at time t . The expectation value is taken with respect to the fields’ quantum state ψ , which drives the two-photon transition. The second term in equation (1) introduces a Lagrangian multiplier λ to enforce the constraint that the product of the mean photon numbers be N^2 photons, with the photon number operator given by $\hat{n}_j = \int d\omega \hat{E}_j^\dagger(\omega) \hat{E}_j(\omega)$. This peculiar normalization separates the well-known linear scaling of the two-photon absorption rate [29] of entangled photons from the impact of quantum correlations: by construction, a separable two-photon state is normalized just like a classical pulse, so any changes in the excitation probability $p_f(t)$ must stem from quantum correlations.

Since we focus on the interaction with weak fields, we obtain $p_f(t)$ perturbatively,

$$\langle \hat{p}_f(t) \rangle_\psi = \langle \hat{T}_{fg}^\dagger(t) \hat{T}_{fg}(t) \rangle, \quad (2)$$

where, at second order in the perturbation, the transition amplitude between g and f reads [35]

$$\hat{T}_{fg}(t) = \int d\omega_a \int d\omega_b T_t(\omega_a, \omega_b) \hat{E}_2(\omega_b) \hat{E}_1(\omega_a),$$

with the function

$$T_t(\omega_a, \omega_b) = \left(\frac{E_0}{\hbar}\right)^2 \sum_e \left(\frac{\mu_{ge}}{\omega_a - \omega_e + i\gamma_e} + \frac{\mu_{ge}}{\omega_b - \omega_e + i\gamma_e} \right) \times \frac{\mu_{ef}}{\omega_a + \omega_b - \omega_f + i\gamma_f} e^{-i(\omega_a + \omega_b)t} \quad (3)$$

describing the matter response to the absorption of photons with frequencies ω_a and ω_b . μ_{ge} and μ_{ef} are the dipole moments connecting adjacent electronic states, γ_e and γ_f are the inverse lifetimes of the respective electronic levels, and E_0 the field normalization [36]. The summation over e includes several possible intermediate states. Our subsequent analysis is restricted to the simplest case of only one single state, but all the results may be straightforwardly generalized to a manifold of e -states. Each excitation of the matter is accompanied by a photon annihilation at the corresponding frequency, rendering equation (2) a field operator acting on the joint space of the two fields 1 and 2.

We further note that, in writing equation (3), we allow for pulses extending infinitely long in time, which simplifies our subsequent discussions. The (more involved) general response for finite interaction times will be given elsewhere. Equation (3) is symmetric with respect to the exchange $\omega_a \leftrightarrow \omega_b$, which means that we assume each field couples to both transitions. In a situation where, for instance, field 1 only drives the g - e transition, and field 2 the e - f transition, we would have to eliminate the second summand in equation (3) to obtain the correct result.

To find the solution of our control problem, we require the first variation of the functional (1) to vanish, $\delta J = 0$, and obtain Fredholm integral equations (see appendix A) which define the optimal pulse forms. This approach may be carried out for arbitrary sample systems. In the present case, when there is a unique target state f , the integral equations may be solved analytically when changing to an appropriate basis of orthogonal functions: as we shall see, this basis is found in the Schmidt decomposition of the matter response function [37]

$$T_t(\omega_a, \omega_b) = \sum_k r_k \psi_k^*(\omega_a) \phi_k^*(\omega_b), \quad (4)$$

where $\{\psi_k\}$ and $\{\phi_k\}$ are orthonormal basis sets, and the r_k are real weights, which may be chosen positive.

3. Classical versus quantum light

We first consider the excitation by multimode coherent states with low mean photon number. Since the field correlation function in $\langle p_f(t) \rangle_\psi$ is normally ordered [38], we may replace the field operators in equation (2) by the field amplitudes [36]

$$\hat{E}_1(\omega_a) \rightarrow A_1(\omega_a), \quad (5)$$

and

$$\hat{E}_2(\omega_b) \rightarrow A_2(\omega_b), \quad (6)$$

such that—for this two-photon process—the light states behave like classical light fields with amplitudes $A_1(\omega_a)$ and $A_2(\omega_b)$. This justifies why, in the following, we shall refer to them as weak, ‘classical’ light pulses. The optimal frequency distributions A_1 and A_2 , equations (A.6) and (A.7), are given by the eigenfunctions pertaining to the largest singular value r_1 in equation (4), i.e. $A_1 = \sqrt{N} \psi_1$ and $A_2 = \sqrt{N} \phi_1$. Using the orthonormality of the Schmidt basis $\{\psi_k\}$ and $\{\phi_k\}$, we may readily carry out the frequency integrations in equation (2), and the maximal classical probability to excite the target state f at time t then reads

$$p_{f,\text{classical}}(t) = N^2 r_1^2. \quad (7)$$

While this maximal probability is time-independent, the ideal solutions A_1 and A_2 depend on the final time t through the time dependence of T_t in equation (4). As we show in the appendix A.1, a mixture of classical states (i.e. classical correlations) cannot enhance the probability any further.

The simple factorization of the four-point field correlation function $\langle \hat{E}_1^\dagger(\omega'_a) \hat{E}_2^\dagger(\omega'_b) \hat{E}_2(\omega_b) \hat{E}_1(\omega_a) \rangle$ in equation (2) into products of field amplitudes, as implied by equations (5) and (6), is no longer possible when describing general quantum states of the field. In particular, when dealing with a general two-photon state, we need to replace $\hat{E}_2(\omega_b) \hat{E}_1(\omega_a)$ by the so-called ‘two-photon wavefunction’ [29, 37]

$$\phi_{\text{quantum}}(\omega_a, \omega_b) = \langle 0 | \hat{E}_2(\omega_b) \hat{E}_1(\omega_a) | \psi \rangle, \quad (8)$$

which describes the transition amplitude from the initial state $|\psi\rangle$ to the vacuum $|0\rangle$, upon absorption of photons at frequencies ω_a and ω_b , respectively. The variation of ϕ_{quantum} (see appendix A.2) yields the optimal two-photon state

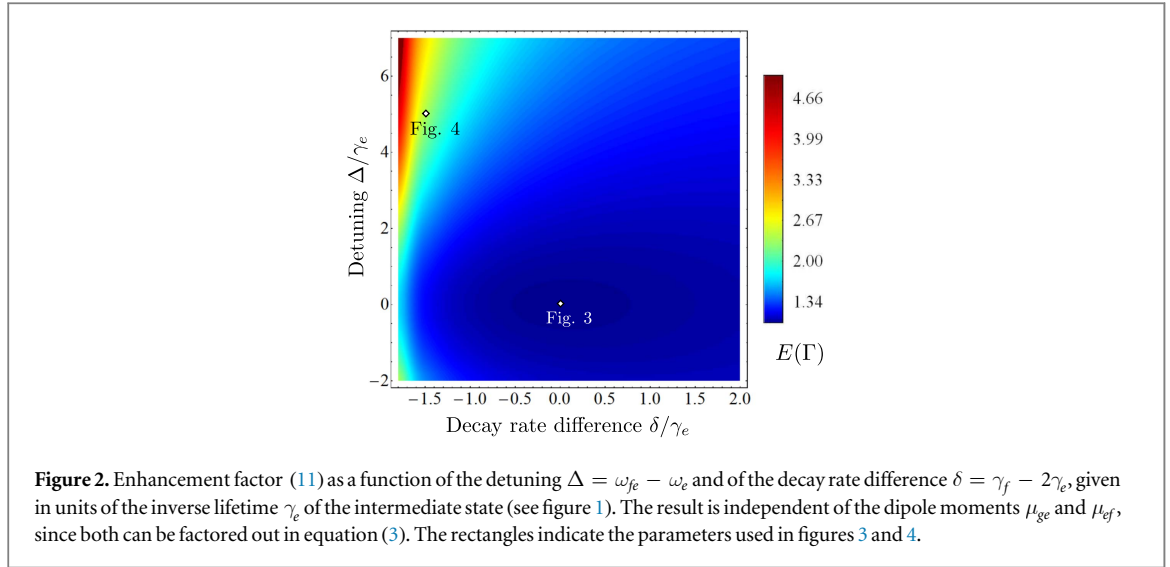


Figure 2. Enhancement factor (11) as a function of the detuning $\Delta = \omega_f - \omega_e$ and of the decay rate difference $\delta = \gamma_f - 2\gamma_e$, given in units of the inverse lifetime γ_e of the intermediate state (see figure 1). The result is independent of the dipole moments μ_{ge} and μ_{ef} , since both can be factored out in equation (3). The rectangles indicate the parameters used in figures 3 and 4.

$$|\psi\rangle = \frac{1}{\sqrt{\mathcal{N}}} \int d\omega_a \int d\omega_b T_i^*(\omega_a, \omega_b) |\omega_a, \omega_b\rangle, \quad (9)$$

where \mathcal{N} is the normalization constant. The state may be visualized as the time-reversed field emitted by the system in a two-photon decay $f \rightarrow g$, similar to the two-level atoms studied in [39–41]. The ideal excitation probability induced by equation (9) reads

$$p_{f,\text{quantum}}(t) = \sum_{k=1}^{\infty} r_k^2. \quad (10)$$

To compare classical and quantum results directly, we divide the classical result, equation (7) by the squared mean photon number N^2 . Equations (7) and (10) then demonstrate that, in principle, entangled photons may be tuned such that they drive resonant two-photon absorption processes more effectively than classical laser pulses. Due to the joint wavefunction, the phase of each pair of frequency components (ω_a, ω_b) in equation (9) is tuned such that the corresponding transition amplitudes—given by equation (3)—sum up constructively. With classical light (6), the phases of ω_a and ω_b are determined independently, thus limiting the transition probability.

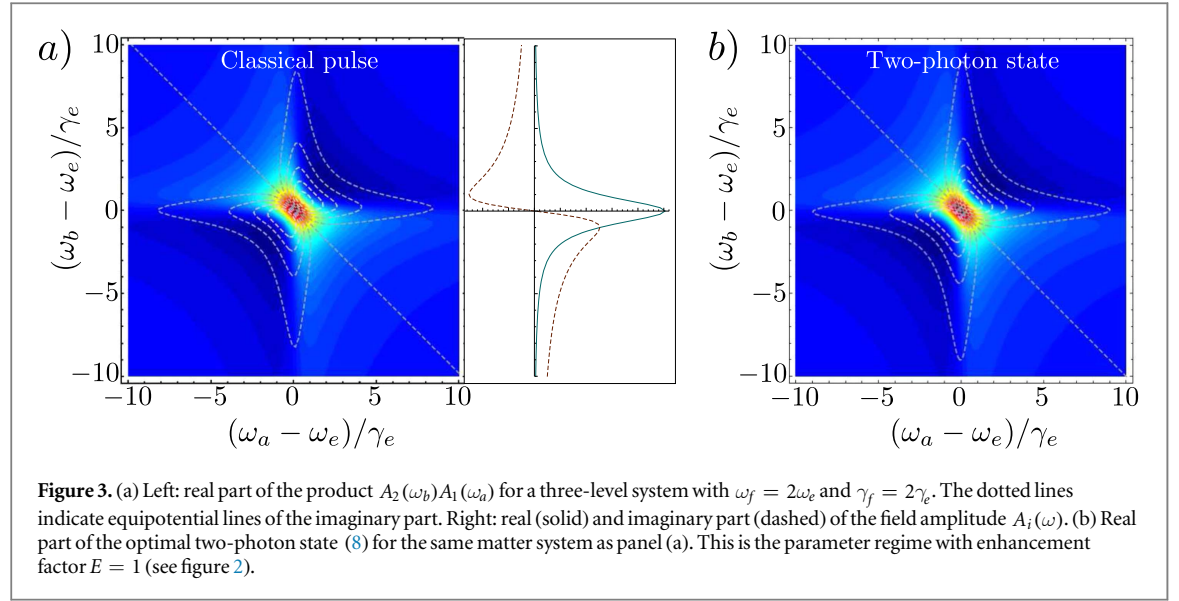
As a specific example, let us consider excitation along the states $5S_{1/2} \rightarrow 5P_{3/2} \rightarrow 5D_{5/2}$ in rubidium, with $\omega_e = 2\pi \times 3.84 \times 10^{14}$ Hz, $\gamma_e^{-1} = 26$ ns, $\omega_f = \omega_e + 2\pi \times 3.86 \times 10^{14}$ Hz, and $\gamma_f^{-1} = 232$ ns [42]. This particular level scheme was already used in [28] to study the influence of the spectral envelope of laser pulses on the two-photon absorption, and for a similar three-state ladder in rubidium in [27] to investigate the absorption of entangled photon pairs. We obtain the rather remarkable ratio $p_{f,\text{quantum}}(t)/p_{f,\text{classical}}(t) \gtrsim 8.9$. In the dimensionless units of figure 2, this corresponds to $\gamma_f/\gamma_e = 0.1$ and, more importantly, $\Delta/\gamma_e = (\omega_f - 2\omega_e)/\gamma_e \sim 10^6$.

These findings naturally lead to the question *under which circumstances* quantum light can be more efficient than classical light. To this end, we investigate the enhancement factor

$$E(\Gamma) \equiv \frac{p_{f,\text{quantum}}(t)}{p_{f,\text{classical}}(t)} = 1 + \frac{1}{r_1^2} \sum_{k=2}^{\infty} r_k^2, \quad (11)$$

where Γ denotes the set of parameters which enter in equation (3). We evaluate $E(\Gamma)$ as a function of the detuning $\Delta = \omega_f - 2\omega_e$ of the e - f transition from the g - e transition, and of the deviation $\delta = \gamma_f - 2\gamma_e$ of the inverse lifetime of the target state from twice the intermediate state's lifetime. The reason behind this peculiar choice of coordinates becomes evident in figure 2: the enhancement factor $E(\Gamma)$ forms a convex function of its arguments Δ and δ , which takes its unique minimum value $E = 1$ (i.e. no enhancement compared to excitation by classical pulses) at $\Delta = \delta = 0$.

To understand this minimum, we note that we can rewrite the two-photon response function for $\Delta = \delta = 0$ as a product of Lorentzian response functions,



$$\left[\frac{1}{\omega_a - \omega_e + i\gamma_e} + \frac{1}{\omega_b - \omega_e + i\gamma_e} \right] \frac{1}{\omega_a + \omega_b - 2\omega_e + i2\gamma_e} = \frac{1}{(\omega_a - \omega_e + i\gamma_e)(\omega_b - \omega_e + i\gamma_e)}. \quad (12)$$

These Lorentzian factors can be interpreted as single-photon response functions for the transition $g \rightarrow e$, for which the transition amplitude in first-order perturbation theory reads [35]

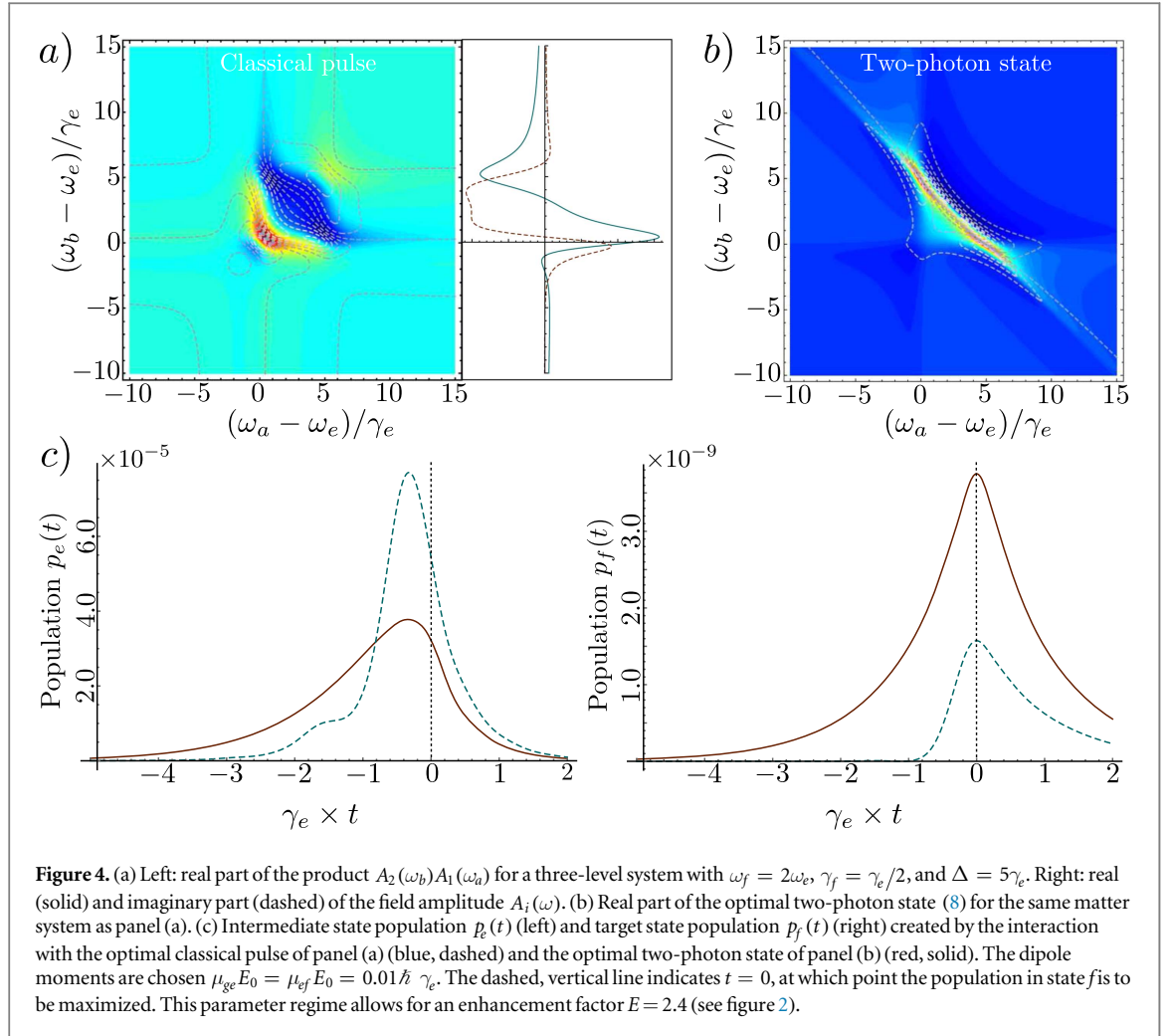
$$T_{eg}(t) = \frac{E_0}{\hbar} \int d\omega \frac{\mu_{eg}}{\omega - \omega_e + i\gamma_e} e^{-i\omega t} A(\omega). \quad (13)$$

Here, the amplitude $A(\omega)$ may describe, both, a classical field amplitude or a single-photon spectral envelope. Hence, at $\Delta = \delta = 0$ the two-photon response function factorizes into the product of single-photon response functions, and no correlations between the first and the second absorption event can induce any quantum advantage (compare equation (9)). Such a situation occurs, for instance, when the sample system consists of noninteracting two-level atoms, for which entangled two-photon absorption was investigated in [43–45]: it was conjectured in [43] that entanglement may enhance two-photon absorption. Our present analysis shows, however, that entanglement cannot enhance the efficiency of the two-photon absorption process in such systems beyond the classical limit: if we consider two two-level atoms with transition frequencies ω_e and $\omega_{e'}$, and each photon interacts with only one of the two-level atoms, we can modify equation (12) to write

$$\frac{1}{(\omega_a - \omega_e + i\gamma_e)(\omega_b - \omega_{e'} + i\gamma_{e'})} = \left[\frac{1}{\omega_a - \omega_e + i\gamma_e} + \frac{1}{\omega_b - \omega_{e'} + i\gamma_{e'}} \right] \frac{1}{\omega_a + \omega_b - \omega_e - \omega_{e'} + i(\gamma_e + \gamma_{e'})}. \quad (14)$$

The two-photon response again factorizes, and there can be no enhancement beyond the classical limit due to photonic entanglement. By comparing optimal pulse forms rather than specific models of light in [43–45], our analysis unambiguously settles this debate.

Since the above discussion also establishes that entangled photons indeed can enhance the two-photon transition probability when either $\Delta \neq 0$ or $\delta \neq 0$, we next investigate the optimal pulse forms in detail. Figure 3 depicts the optimal classical field amplitudes $A_2(\omega_b)A_1(\omega_a)$ (panel (a)) and two-photon wavefunction $\phi(\omega_a, \omega_b)$ (panel (b)) at the minimum in figure 2, i.e. when the two-photon transition amplitude factorizes as in equation (12). Clearly, the two pulse forms are identical, as was clear from our theoretical analysis. Since in our present study equation (3) was chosen symmetric with respect to the exchange $\omega_a \leftrightarrow \omega_b$, so are the two field amplitudes, i.e. $A_1 = A_2$, and it is sufficient to show one of them in the right inset of panel (a). It is simply given by a Lorentzian lineshape $\sim 1/(\omega - \omega_e - i\gamma_e)$, i.e. in the time domain by a ‘rising exponential’ shape. This behavior was to be expected from previous results on single-photon excitation of a two-level atom [39–41], where a ‘rising exponential’ temporal shape was shown to couple most efficiently to the matter system. In the case of noninteracting two-level atoms, it is quite intuitive that this pulse shape is still optimal for two-photon excitations, when the two absorption events are not correlated.



The situation changes substantially when the two-photon state does enhance the transition probability: in figure 4, we depict the case where the second transition energy is larger than the first one, with $\Delta = 5\gamma_e$, and the target state lives longer than the intermediate state, $\gamma_f = \gamma_e/2$ (as was also the case in our rubidium example above): the optimal classical pulses (panel (a)) show a broad structure in the area $(\omega_a, \omega_b) \in (\omega_e \dots \omega_e + \Delta, \omega_e \dots \omega_e + \Delta)$. While, at first glance, these optimal pulses appear very different from the harmonic case before, this structure can still be understood by the interference of three Lorentzians: in addition to the harmonic Lorentzian of figure 3, one more Lorentzian contributes for, each, the nonvanishing Δ and δ .

In contrast, the optimal entangled wavefunction (panel (b)) forms a narrow structure along the anti-diagonal. Its width along the diagonal becomes a lot narrower than in figure 3(a), reflecting the narrow linewidth of the target state γ_f , whereas the width along the anti-diagonal remains the same, since the lifetime of the intermediate state is unaltered. Due to the detuning Δ of the e - f transition, it acquires a double peak structure with maxima at $(\omega_a, \omega_b) = (\omega_e, \omega_e + \Delta)$, and at $(\omega_e + \Delta, \omega_e)$, such that the sum of the two frequencies always matches ω_f . In contrast to the classical pulses in panel (a), the two-photon wavefunction shows no intensity at (ω_e, ω_e) , nor at $(\omega_e + \Delta, \omega_e + \Delta)$. This is only possible in the quantum regime, since the absorption of the first photon affects the wavefunction of the other photon, thereby influencing the second absorption event [46]. The two-photon wavefunction is a clear indicator of strong frequency anticorrelations in the pure two-photon state considered here [37, 47, 48], and it is these correlations that are responsible for the 140% enhancement ($E = 2.4$) of the quantum transition probability.

To see how the spectral structures of the optimal pulses affect the absorption process, we simulate the time evolution of the excited state populations $p_e(t)$ (left) and $p_f(t)$ (right) in panel (c) of figure 4 [49]. Clearly, while the maximal population in the intermediate state p_e is larger for the case of classical pulses, the maximal target state population $p_f(t = 0)$ upon absorption of entangled pairs exceeds the ‘classical’ optimal population by a 1.4-fold—as predicted by the enhancement factor (11) for the current set of parameters.

The broad bandwidth of the classical pulses is reflected in a steep rise of both the intermediate and target state populations near $t = 0$. The intermediate state e decays more rapidly than the target state f , such that the optimal classical pulse has to strongly excite this state shortly before the population in f shall be maximized.

In contrast, the populations induced by the absorption of entangled photons rise much slower. Since frequency-anticorrelated photons arrive in pairs [21], the time the system spends in the intermediate state is minimized. It further means that at any point in time there is a finite probability to find the system in the intermediate state. This driving causes a perfectly symmetric progression of the target state population $p_f(t)$ which rises with the same speed it subsequently decays again. This could be anticipated from the optimal state (9) which is given by the complex conjugate (hence, the time-reverse) of the matter response (3). The inability of the classical pulses to reproduce this symmetric time evolution lies at the heart of the quantum advantage discussed here.

4. Summary and outlook

We investigated optimal pulse forms to efficiently drive a resonant two-photon transition with weak fields. Our study represents—to the best of our knowledge—the first theoretical investigation of coherent control theory in the presence of quantum correlations. Whereas previous studies on coherent control with quantum light focus on the manipulation of interference between excitation pathways [22], where the quantum properties of light may in fact be detrimental, our study shows that photonic entanglement potentially renders the two-photon absorption process significantly more efficient than classical pulses—except for two-photon absorption in noninteracting systems. Such shaping of the two-photon wavefunction provides a useful application of entangled photons as a spectroscopic probe of photosensitive samples where large photon fluxes are to be avoided [50–52].

Our introduction of the Schmidt decomposition—a concept from quantum information theory—to analyze the material response function could have applications well beyond the simple systems considered here, as it offers a new perspective on the nonlinear response of (possibly complex) quantum systems. The Schmidt coefficients—very much like in the case of photonic entanglement, where they determine the effective dimension of the Hilbert space available for quantum information purposes [37]—contain information about couplings between resonances in the quantum system. The current approach extracts this information from the optical response of the system, and could thus provide a tool to analyze entanglement with optical measurements, for instance, the interaction-induced entanglement of excitons in complex systems [53].

Future work could investigate the impact of quantum correlations beyond the perturbative limit to analyze experiments such as those carried out by the Sandoghdar [1–3], or the Leuchs groups [54, 55], and beyond the two-photon limit when incoherent contributions need to be taken into account [31]. Furthermore, we have not considered off-resonant two-photon transitions in this manuscript. We believe however that our formalism could be expanded to include off-resonant intermediate states by imposing additional constraints in the functional (1).

Acknowledgments

We would like to acknowledge helpful discussions with Stefan Lerch and André Stefanov, which stimulated the current manuscript. FS would like to thank the German National Academic Foundation for support, and acknowledges financial support of the European Research Council under the European Union's Seventh Framework Programme (FP7/2007-2013)/ERC Grant Agreement No. 319286 Q-MAC. AB thanks Dieter Jaksch and Keble College Oxford for hospitality. FS and AB acknowledge partial funding by the German Academic Exchange Service (DAAD).

Appendix A. Integral equations

A.1. Classical fields

If the matter system is excited by classical fields with envelopes A_1 and A_2 , the field operators are replaced by the classical amplitudes (see equations (5) and (6)). Equation (1) then reads

$$J[A_1, A_2] = \int d\omega_a \int d\omega_b \int d\omega'_a \int d\omega'_b T_t(\omega'_a, \omega'_b) T_t^*(\omega_a, \omega_b) A_1(\omega'_a) A_2(\omega'_b) A_1^*(\omega_a) A_2^*(\omega_b) - \lambda \left[\int d\omega_a |A_1(\omega_a)|^2 \int d\omega_b |A_2(\omega_b)|^2 - N^2 \right]. \quad (\text{A.1})$$

Requiring the variation of equation (A.12) to vanish for arbitrary changes δA_1 and δA_2 around the optimal pulse forms, we must impose that linear terms in δA_1 and δA_2 vanish identically, $\int d\omega_a \delta A_1(\omega_a) [\dots] \equiv 0$. This yields the coupled, nonlinear integral equations (the variation of the complex conjugate amplitudes δA_1^* and δA_2^* yields the complex conjugate integral equations)

$$A_1(\omega_a) = \frac{1}{\int d\omega |A_2(\omega)|^2} \int d\omega_b \int d\omega'_a \int d\omega'_b K(\omega_a, \omega_b; \omega'_a, \omega'_b) A_2^*(\omega_b) A_2(\omega'_b) A_1(\omega'_a), \quad (\text{A.2})$$

$$A_2(\omega_b) = \frac{1}{\int d\omega |A_1(\omega)|^2} \int d\omega_a \int d\omega'_a \int d\omega'_b K(\omega_a, \omega_b; \omega'_a, \omega'_b) A_1^*(\omega_a) A_2(\omega'_b) A_1(\omega'_a), \quad (\text{A.3})$$

with the kernel

$$K(\omega_a, \omega_b; \omega'_a, \omega'_b) = \frac{1}{\lambda} T_t(\omega'_a, \omega'_b) T_t^*(\omega_a, \omega_b). \quad (\text{A.4})$$

The variation of the Lagrange multiplier, $\partial J[A_1, A_2]/\partial \lambda \equiv 0$, similarly yields the normalization condition

$$\int d\omega_a |A_1(\omega_a)|^2 \int d\omega_b |A_2(\omega_b)|^2 = N^2. \quad (\text{A.5})$$

Using the Schmidt decomposition (4) of the matter response function, it becomes apparent that

$$A_1^{(k)}(\omega_a) = \sqrt{N} \psi_k(\omega_a), \quad (\text{A.6})$$

$$A_2^{(k)}(\omega_b) = \sqrt{N} \phi_k(\omega_b) \quad (\text{A.7})$$

are solutions of the integral equations. Hence, the solutions pertaining to the largest Schmidt eigenvalue r_1 maximize the classical two-photon absorption within this set of solutions. Strictly speaking, we do not need to assume identical amplitudes in each beam. Any pair $(\sqrt{Na} \psi_k, \sqrt{N/a} \phi_k)$ for $a \in (0, 1)$ also solves the integral equations. However, in the low-intensity regime considered here this reshuffling of amplitude between the two beams does not add any new physics to the problem, so we restrict our attention to solutions (A.6) and (A.7).

A.1.1. Maximality of the solutions. This section proves that the solutions $A_1^{(1)}$ and $A_2^{(1)}$ are in fact the optimal classical pulse forms.

Suppose there are different solutions $\tilde{A}_1(\omega)$ and $\tilde{A}_2(\omega)$ of equations (A.2) and (A.3). Since the basis sets $\{\psi_k\}$ and $\{\phi_k\}$ each form complete sets of orthogonal functions, we may expand $\tilde{A}_1(\omega) = \sqrt{N} \sum_k c_k \psi_k(\omega)$ and $\tilde{A}_2(\omega) = \sqrt{N} \sum_k d_k \phi_k(\omega)$. The normalization of the field contribution in equation (1) yields (for simplicity, we only consider the case $N = 1$) $\sum_k |c_k|^2 = \sum_k |d_k|^2 = 1$, and the two-photon amplitude, upon insertion of the solutions (A.6) and (A.7) into the transition amplitude (2)

$$\begin{aligned} p_f(t) &= |N \sum_k r_k c_k d_k|^2 \leq \left(N \sum_k r_k |c_k| |d_k| \right)^2 \\ &\leq N^2 r_1^2 \left(\sum_k |c_k| |d_k| \right)^2, \end{aligned} \quad (\text{A.8})$$

where we have used the triangle inequality in the first estimation. To proceed, we invoke the Hölder inequality [56]

$$\sum_k |x_k y_k| \leq \left(\sum_k |x_k|^p \right)^{1/p} \left(\sum_k |y_k|^q \right)^{1/q}, \quad (\text{A.9})$$

to write (with $p = q = 2$),

$$p_f(t) \leq N^2 r_1^2 \sum_k |c_k|^2 \sum_k |d_k|^2 = N^2 r_1^2, \quad (\text{A.10})$$

where we recall $N^2 r_1^2$ is the optimal result (7) of the pulses $A_1^{(1)}$ and $A_2^{(1)}$. Hence, $A_1^{(1)}$ and $A_2^{(1)}$ are indeed the optimal solutions.

Similarly, an incoherent mixture of different eigenfunctions ψ_k and ϕ_k with weights \tilde{p}_k cannot enhance the maximal transition probability (7): we obtain

$$p_f(t) = N^2 \sum_k \tilde{p}_k r_k^2 \leq N^2 r_1^2 \sum_k \tilde{p}_k = N^2 r_1^2. \quad (\text{A.11})$$

A.2. Photon pairs

In case the initial state of the light field ψ is given by a two-photon state, the field enters in equation (2) with its two-photon wavefunction, $\phi(\omega_a, \omega_b) = \langle 0 | E(\omega_b) E(\omega_a) | \psi \rangle$ (see equation (8)). The functional (1) is then given

Table B1. Convergence of the numerical evaluation of equation (B.1) with $\omega_f = 2\omega_e$ and $\gamma_f = 2\gamma_e$. From our analysis of equation (9) we know that $E = 1$.

Grid size	Grid resolution	$E(\gamma_f = 2\gamma_e)$
$\pm 100\gamma_f$	$\gamma_e/5$	0.996 819
$\pm 100\gamma_f$	$\gamma_e/10$	0.996 818
$\pm 200\gamma_f$	$\gamma_e/5$	0.998 409
$\pm 200\gamma_f$	$\gamma_e/10$	0.998 409
$\pm 300\gamma_f$	$\gamma_e/5$	0.998 939
$\pm 350\gamma_f$	$\gamma_e/5$	0.999 091

by

$$J[\phi] = \int d\omega_a \int d\omega_b \int d\omega'_a \int d\omega'_b T_t(\omega'_a, \omega'_b) T_t^*(\omega_a, \omega_b) \phi(\omega'_a, \omega'_b) \phi^*(\omega_a, \omega_b) - \lambda \left[\int d\omega_a \int d\omega_b |\phi(\omega_a, \omega_b)|^2 - 1 \right]. \quad (\text{A.12})$$

In an analogous calculation to the derivation of equations (A.2) and (A.3), we require the variation of the functional to vanish for arbitrary changes $\delta\phi$ around the optimal solution. We then obtain the homogeneous Fredholm equation [56]

$$\phi(\omega_a, \omega_b) = \int d\omega'_a \int d\omega'_b K(\omega_a, \omega_b; \omega'_a, \omega'_b) \phi(\omega'_a, \omega'_b), \quad (\text{A.13})$$

with the kernel given in equation (A.4), which determines the optimal two-photon wavefunction, with the normalization

$$\int d\omega_a \int d\omega_b |\phi(\omega_a, \omega_b)|^2 = 1. \quad (\text{A.14})$$

It is solved by

$$\phi_{\max}(\omega_a, \omega_b) = \frac{1}{\sqrt{\mathcal{N}}} \sum_k r_k \psi_k(\omega_a) \phi_k(\omega_b) \quad (\text{A.15})$$

with the (state) normalization

$$\mathcal{N} = \int d\omega_a \int d\omega_b |T_t(\omega_a, \omega_b)|^2 \quad (\text{A.16})$$

$$= \frac{2\pi(\mu_{ge}E_0)^2(\mu_{ef}E_0)^2}{\hbar^4\gamma_e\gamma_f}. \quad (\text{A.17})$$

This corresponds to the two-photon state (8) in the main text.

The state normalization also represents the maximal population in the target state f . Using equation (A.15), the population $p_f(t)$ reads

$$p_f(t) = |T_{fg}|^2 = \frac{1}{\mathcal{N}} |T_t^*(\omega_a, \omega_b)|^2 = \mathcal{N}. \quad (\text{A.18})$$

Appendix B. Schmidt decomposition

Following [37], the singular values, and the eigenfunctions of the Schmidt decomposition (4) may be obtained numerically by solving the eigenvalue equation

$$\int d\omega' \kappa(\omega, \omega') \psi_k(\omega') = r_k^2 \psi_k(\omega), \quad (\text{B.1})$$

with the kernel

$$\kappa(\omega, \omega') = \int d\omega'' T_{t;t_0}^*(\omega, \omega'') T_{t;t_0}(\omega', \omega''). \quad (\text{B.2})$$

The integral equation (B.1) was solved numerically in Mathematica by discretizing the frequency space into a grid in the range $\omega - \omega_e \in [-100 \times \max(\gamma_e, \gamma_f), 100 \times \max(\gamma_e, \gamma_f)]$, with a step size of $\min(\gamma_e, \gamma_f)/5$. This step size was chosen to obtain with confidence the largest eigenvectors, which vary only weakly between

adjacent grid points. The eigenvectors pertaining to larger eigenvalues r_k^2 rapidly start to oscillate with the frequency, which may necessitate an enhanced frequency resolution. Note further that due to the long tails of the resulting Lorentzian pulse shapes very large frequency ranges need to be sampled to obtain a convergent result.

We used the optimal quantum state (9) as a reference: according to our previous analysis, the optimal population in the target state f induced by quantum light has to coincide with the numerical result for r_1^2 from equation (B.1), if $\gamma_f = 2\gamma_e$ and $\omega_f = 2\omega_e$. We obtain the numerical values for different grid sizes shown in table B1.

We note that, to obtain the largest eigenvalue of equation (B.1), an increase of the step size beyond $\gamma_e/5$ only changes the result by on the order of 10^{-6} for a grid size of $\pm 100\gamma_f$, and even less for $\pm 200\gamma_f$. Instead, to enhance the numerical precision, it is necessary to sample a very large area around the central frequencies, in order to cover the very large tails of the Lorentzian distribution to a sufficient extent.

References

- [1] Pototschnig M *et al* 2011 Controlling the phase of a light beam with a single molecule *Phys. Rev. Lett.* **107** 063001
- [2] Rezus Y L A *et al* 2012 Single-Photon spectroscopy of a single molecule *Phys. Rev. Lett.* **108** 093601
- [3] Faez S, Türschmann P, Haakh H R, Götzinger S and Sandoghdar V 2014 Coherent interaction of light and single molecules in a dielectric nanoguide *Phys. Rev. Lett.* **113** 213601
- [4] Hildner R *et al* 2013 Quantum coherent energy transfer over varying pathways in single light-harvesting complexes *Science* **340** 1448–51
- [5] Walschaers M, Diaz J F, Mulet R and Buchleitner A 2013 Optimally designed quantum transport across disordered networks *Phys. Rev. Lett.* **111** 180601
- [6] Skourtis S S, Waldeck D H and Beratan D N 2010 Fluctuations in biological and bioinspired electron-transfer reactions *Ann. Rev. Phys. Chem.* **61** 461–85
- [7] Peyronel T *et al* 2012 Quantum nonlinear optics with single photons enabled by strongly interacting atoms *Nature* **488** 57–60
- [8] Chen W *et al* 2013 All-optical switch and transistor gated by one stored photon *Science* **341** 728–70
- [9] Shomroni I *et al* 2014 All-optical routing of single photons by a one-atom switch controlled by a single photon *Science* **345** 903–6
- [10] Firstenberg O *et al* 2013 Attractive photons in a quantum nonlinear medium *Nature* **502** 71–5
- [11] Baur S, Tiarks D, Rempe G and Dürr S 2014 Single-photon switch based on Rydberg blockade *Phys. Rev. Lett.* **112** 073901
- [12] Tiarks D, Baur S, Schneider K, Dürr S and Rempe G 2014 Single-photon transistor using a Förster resonance *Phys. Rev. Lett.* **113** 053602
- [13] Raimond J M, Brune M and Haroche S 2001 Manipulating quantum entanglement with atoms and photons in a cavity *Rev. Mod. Phys.* **73** 565–82
- [14] Wather H, Varcoe B T H, Englert B-G and Becker T 2006 Cavity quantum electrodynamics *Rep. Prog. Phys.* **69** 1325
- [15] Schwartz T, Hutchison J A, Genet C and Ebbesen T W 2011 Reversible switching of ultrastrong light-molecule coupling *Phys. Rev. Lett.* **106** 196405
- [16] He B, Sharypov A V, Sheng J, Simon C and Xiao M 2014 Two-photon dynamics in coherent Rydberg atomic ensemble *Phys. Rev. Lett.* **112** 133606
- [17] Gorniaczyk H, Tresp C, Schmidt J, Fedder H and Hofferberth S 2014 Single-photon transistor mediated by interstate Rydberg interactions *Phys. Rev. Lett.* **113** 053601
- [18] Loo V *et al* 2012 Optical nonlinearity for few-photon pulses on a quantum dot-pillar cavity device *Phys. Rev. Lett.* **109** 166806
- [19] Castet F *et al* 2013 Design and characterization of molecular nonlinear optical switches *Acc. Chem. Res.* **46** 2656–65
- [20] Assion A *et al* 1998 Control of chemical reactions by feedback-optimized phase-shaped femtosecond laser pulses *Science* **282** 919–22
- [21] Meshulach D and Silberberg Y 1999 Coherent quantum control of multiphoton transitions by shaped ultrashort optical pulses *Phys. Rev. A* **60** 1287–92
- [22] Shapiro J H and Brumer P 2012 *Quantum Control of Molecular Processes* (Hoboken: Wiley)
- [23] Lukens J M *et al* 2013 Biphoton manipulation with a fiber-based pulse shaper *Opt. Lett.* **38** 4652–5
- [24] Bernhard C, Bessire B, Feurer T and Stefanov A 2013 Shaping frequency-entangled qubits *Phys. Rev. A* **88** 032322
- [25] Bessire B, Bernhard C, Feurer T and Stefanov A 2014 Versatile shaper-assisted discretization of energy-time entangled photons *New J. Phys.* **16** 033017
- [26] Defienne H *et al* 2016 Two-photon quantum walk in a multimode fiber *Sci. Adv.* **2** e1501054
- [27] Dayan B, Pe'er A, Friesem A A and Silberberg Y 2004 Two photon absorption and coherent control with broadband down-converted light *Phys. Rev. Lett.* **93** 023005
- [28] Dudovich N, Dayan B, Faeder S M G and Silberberg Y 2001 Transform-limited pulses are not optimal for resonant multiphoton transitions *Phys. Rev. Lett.* **86** 47–50
- [29] Javanainen J and Gould P L 1990 Linear intensity dependence of a two-photon transition rate *Phys. Rev. A* **41** 5088–91
- [30] Grice W P, U'Ren A B and Walmsley I A 2001 Eliminating frequency and space-time correlations in multiphoton states *Phys. Rev. A* **64** 063815
- [31] Dayan B 2007 Theory of two-photon interactions with broadband down-converted light and entangled photons *Phys. Rev. A* **76** 043813
- [32] Bea-Banacloche J 1989 Two-photon absorption of nonclassical light *Phys. Rev. Lett.* **62** 1603
- [33] Georgiades N P *et al* 1995 Nonclassical excitation for atoms in a squeezed vacuum *Phys. Rev. Lett.* **75** 3426
- [34] Georgiades N P, Polzik E S and Kimble H J 1997 Atoms as nonlinear mixers for detection of quantum correlations at ultrahigh frequencies *Phys. Rev. A* **55** R1605
- [35] Cohen-Tannoudji C and Guéry-Odelin D 2011 *Advances In Atomic Physics: An Overview* (Singapore: World Scientific)
- [36] Mandel L and Wolf E 1995 *Optical Coherence and Quantum Optics* (Cambridge: Cambridge University Press)
- [37] Law C K, Walmsley I A and Eberly J H 2000 Continuous frequency entanglement: effective finite hilbert space and entropy control *Phys. Rev. Lett.* **84** 5304–7
- [38] Mollow B R 1968 Two-photon absorption and field correlation functions *Phys. Rev.* **175** 1555–63
- [39] Stobinská M, Alber G and Leuchs G 2009 Perfect excitation of a matter qubit by a single photon in free space *Europhys. Lett.* **86** 14007
- [40] Wang Y, Minář J, Sheridan L and Scarani V 2011 Efficient excitation of a two-level atom by a single photon in a propagating mode *Phys. Rev. A* **83** 063842

- [41] Aljunid S A *et al* 2013 Excitation of a single atom with exponentially rising light pulses *Phys. Rev. Lett.* **111** 103001
- [42] Safronova M S and Safronova U I 2011 Critically evaluated theoretical energies, lifetimes, hyperfine constants, and multipole polarizabilities in ^{87}Rb *Phys. Rev. A* **83** 052508
- [43] Muthukrishnan A, Agarwal G S and Scully M O 2004 Inducing disallowed two-atom transitions with temporally entangled photons *Phys. Rev. Lett.* **93** 093002
- [44] Richter M and Mukamel S 2011 Collective two-particle resonances induced by photon entanglement *Phys. Rev. A* **83** 063805
- [45] Zheng Z, Saldanha P L, Rios Leite J R and Fabre C 2013 Two-photon two-atom excitation by correlated light states *Phys. Rev. A* **88** 033822
- [46] Schlawin F and Mukamel S 2014 Matter correlations induced by coupling to quantum light *Phys. Rev. A* **89** 013830
- [47] Cho Y-W, Park K-K, Lee J-C and Kim Y-H 2014 Engineering frequency–time quantum correlation of narrow-band biphotons from cold atoms *Phys. Rev. Lett.* **113** 063602
- [48] Franson J D 1989 Bell inequality for position and time *Phys. Rev. Lett.* **62** 2205–8
- [49] Oka H 2010 Real-time analysis of two-photon excitation by correlated photons: pulse-width dependence of excitation efficiency *Phys. Rev. A* **81** 053837
- [50] Upton L *et al* 2013 Optically excited entangled states in organic molecules illuminate the dark *J. Phys. Chem. Lett.* **12** 2046–52
- [51] Schlawin F, Dorfman K E, Fingerhut B P and Mukamel S 2013 Suppression of population transport and control of exciton distributions by entangled photons *Nat. Commun.* **4** 1782
- [52] Raymer M G, Marcus A H, Widom J R and Vitullo D L P 2013 Entangled photon-pair two-dimensional fluorescence spectroscopy (EPP-2DFS) *J. Phys. Chem. B* **117** 15559–75
- [53] Healion D, Zhang Y, Biggs J D, Govind N and Mukamel S 2012 Entangled valence electron-hole dynamics revealed by stimulated attosecond x-ray Raman scattering *J. Phys. Chem. Lett.* **3** 2326–31
- [54] Maiwald R *et al* 2012 Collecting more than half the fluorescence photons from a single ion *Phys. Rev. A* **86** 043431
- [55] Fischer M *et al* 2014 Efficient saturation of an ion in free space *Appl. Phys. B* **117** 797–801
- [56] Abramowitz M and Stegun A 2012 *Handbook of Mathematical Functions* (Mineola: Dover)